



# Studies on Li–Mn–O spinel system (obtained from melt-impregnation method) as a cathode for 4 V lithium batteries

## Part V. Enhancement of the elevated temperature performance of Li/LiMn<sub>2</sub>O<sub>4</sub> cells

Yongjao Xia, Yasufumi Hideshima, Naoki Kumada, Masamitsu Nagano, Masaki Yoshio \*

*Department of Applied Chemistry, Saga University, Saga 840-8502, Japan*

Received 23 August 1997; revised 18 December 1997

### Abstract

Stoichiometric LiMn<sub>2</sub>O<sub>4</sub>, metal-ion doped (Li<sup>+</sup> and Co<sup>3+</sup>) spinels, Li<sub>1+x</sub>Mn<sub>2-x-y</sub>M<sub>y</sub>O<sub>4</sub>, and fluorine substituted spinel, Li<sub>1+x</sub>Mn<sub>2</sub>O<sub>4-z</sub>F<sub>z</sub>, are examined as cathodes in Li/organic electrolyte/Li<sub>x</sub>Mn<sub>2</sub>O<sub>4</sub> cells containing various electrolytes at both room temperature and 50°C. The elevated temperature performance is improved with the metal-ion doped and fluorine substituted spinels in LiBF<sub>4</sub> base electrolyte solution. © 1998 Elsevier Science S.A. All rights reserved.

*Keywords:* Lithium; Lithium-ion batteries; Spinel; Manganese dioxide; Elevated performance

### 1. Introduction

Spinel Li<sub>x</sub>Mn<sub>2</sub>O<sub>4</sub> has been demonstrated to be the most promising positive electrode material for lithium-ion batteries because it is cheaper, less toxic, and easier to prepare than alternative materials (LiCoO<sub>2</sub> and LiNiO<sub>2</sub>). We have successfully prepared optimum electrode materials from various manganese dioxide and lithium salts by the ‘melt-impregnation method’ [1,2], and have demonstrated the relationship between the capacity and rechargeability of these spinels [3]. The spinel now exhibits excellent performance: it maintains a rechargeable capacity of more than 120 mAh g<sup>-1</sup> over extensive cycling at room temperature. On the other hand, it exhibits poor performance at elevated temperatures; the capacity degrades rapidly with cycling. This is commonly considered to be due to dissolution of Mn into the electrolyte caused by the disproportionation reaction: 2Mn<sup>3+</sup> → Mn<sup>4+</sup> + Mn<sup>2+</sup> [4,5]. Recently, we have demonstrated the failure mechanism in detail [6]. The major factors responsible for the capacity loss at high temperature are described in Fig. 1, namely, (i) the transformation of the unstable two-phase structure on

the high-voltage region to a more stable one-phase structure, accompanied by the loss of MnO; (ii) direct dissolution of Mn<sub>2</sub>O<sub>3</sub> into the electrolyte solution; (iii) decomposition of electrolyte solution on the electrode. Accordingly, several ways are taken in this investigation to improve the elevated temperature performance, e.g., use of metal-ion doped spinels, change of electrolyte with low HF content instead of LiPF<sub>6</sub>, reduced surface area of the electrode material, etc.

### 2. Experimental

The compound examined here was prepared by the melt-impregnation method [1]. The starting materials were LiOH, LiF, MnO<sub>2</sub>, and Co(OH)<sub>3</sub>. The detailed synthesis conditions are given in Section 3.1.

The chemical composition of each compound was analyzed by chemical analysis [7]. The crystal structure was characterized by X-ray diffraction measurement, and the specific surface-area was measured in a Gemini 2375 instrument by the Brunauer, Emmett, and Teller (BET) method.

Charge–discharge tests and cycle-life tests were examined in CR2030 button type cells. The cell consisted of a

\* Corresponding author.

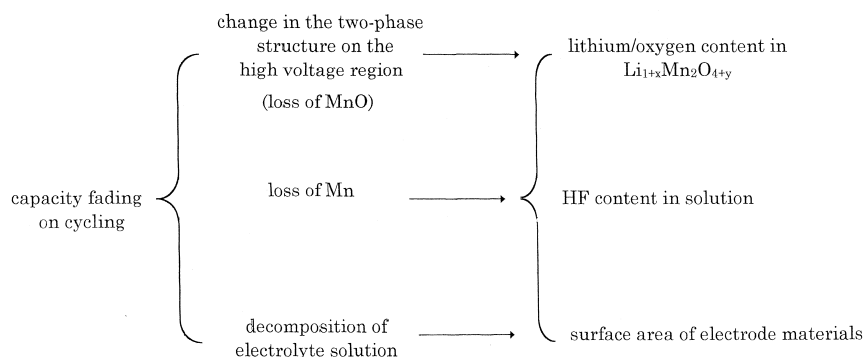


Fig. 1. Factors that affect the elevated-temperature performance of Li/LiMn<sub>2</sub>O<sub>4</sub> cells.

cathode and a lithium metal anode separated by a porous polypropylene film. Metallic lithium was in excess. The mixture, which contained 20 mg of active material and 12 mg of conducting binder, was pressed on 2.0 cm<sup>2</sup> stainless screen at 800 kg cm<sup>-2</sup>, dried and assembled as a cathode in the cell. The cell was cycled at a current rate of  $C/3$  between 3.0 and 4.3 V, unless otherwise specified.

The electrolyte was 1 M LiPF<sub>6</sub>, or LiBF<sub>4</sub> or LiClO<sub>4</sub>-ethylene carbonate (EC)/dimethyl carbonate (DMC) (1:2 in volume). The water content in each solution was less than 20 ppm.

Cyclic voltammetry measurements were carried out in a three-electrode glass cell. Metallic lithium was used for the counter and reference electrodes. All cell assemblies were carried out in a dry box filled with argon gas. Other sets of experimental conditions are given in each Section.

### 3. Results and discussion

#### 3.1. Synthesis

Spinel were prepared by heating a stoichiometric mixture of LiOH (or addition of LiF) and MnO<sub>2</sub> (or doping Co(OH)<sub>3</sub>) at 470°C for 5 h, followed by heating at 530°C for 5 h with a flow of air. Finally, the spinel was heated at various temperatures for 20 h in air, and then slow cooled for 3 h in air. The detailed synthesis conditions are given in Table 1. Analysis of materials by X-ray diffraction revealed that the samples consist of single-phase spinels. The calculated cubic lattice parameters,  $a_0$ , from XRD

patterns, the chemical composition of each compound determined by chemical analysis, and the specific surface-area calculated by the BET method are listed in Table 2. Assuming that the oxidation state of Co in doped spinels is Co<sup>2+</sup> or Co<sup>3+</sup>, e.g., samples C and D, then two possible chemical formulae are given in Table 2. The calculated and measured capacities the samples are also shown in Table 2. The measured data were obtained from Li/LiCo<sub>x</sub>Mn<sub>2-x</sub>O<sub>4</sub> cycled between 3.0 and 4.3 V at a current rate of 0.1 mA cm<sup>-2</sup>. The results show that the measured capacity is close to that calculated when taking the oxidation state of Co in doped spinels as Co<sup>3+</sup>. This suggests that the oxidation of Co is most possibly Co<sup>3+</sup>, which is in agreement with the finding reported in Ref. [8].

#### 3.2. Electrochemical properties

Typical charge and discharge curves for a Li/Li<sub>x</sub>Mn<sub>2</sub>O<sub>4</sub> cell at room temperature containing various spinel cathodes are shown in Fig. 2. The initial capacity of these metal-ion doped (lithium or Co) spinels is slightly lower than that of the stoichiometric spinel LiMn<sub>2</sub>O<sub>4</sub>, which is consistent with the fact that the doped metal ions occupy the 16d octahedral sites and, thereby, reduce the quantity of Mn<sup>3+</sup>. It is expected that substitution of fluorine should result in an increase in specific capacity, as fluorine acts to reduce Mn<sup>4+</sup> to Mn<sup>3+</sup>, but the lithium manganese fluoride examined here, which was prepared at low temperature, is an oxygen-rich compound with an average Mn valence of 3.566. It is of interest to note that the differ-

Table 1  
Sample preparation conditions

Sample No.	Molar ratio	Preparation	Conditions
A	Li/Mn = 0.50	470°C, 5 h; 530°C, 5 h with air flow, cooled and ground	750°C in air, 20 h, cooled in 3 h
B	Li/Mn = 0.525, LiF/LiOH = 0.05		675°C in air, 20 h, cooled in 3 h
C	Li/(Mn + Co) = 0.52, Co/Mn = 0.05/1.95		700°C in air, 20 h, cooled in 3 h
D	Li/(Mn + Co) = 0.55, Co/Mn = 0.05/1.95		650°C in air, 20 h, cooled in 3 h

Table 2  
Physical properties of spinel samples

Sample No.	Composition	Cubic $a$ -axis ( $\text{\AA}$ )	Specific surface area ( $\text{m}^2 \text{g}^{-1}$ )	$C_{\text{theo.}}$ from $\text{Mn}^{3+}$ ( $\text{mAh g}^{-1}$ )	$C_{\text{exp.}}$ ( $\text{mAh g}^{-1}$ )
A	$\text{LiMn}_2\text{O}_4$	8.246	3.6	148	134
B	$\text{Li}_{1.05}\text{Mn}_2\text{F}_{0.05}\text{O}_{4.066}$	8.237	6.2	128	121
C	$\text{Li}_{1.04}\text{Mn}_{1.95}\text{Co(II)}_{0.05}\text{O}_{4.077}$	8.230	4.5	116	124
D	$\text{Li}_{1.04}\text{Mn}_{1.95}\text{Co(III)}_{0.05}\text{O}_{4.053}$	8.220	6.9	103	107
	$\text{Li}_{1.1}\text{Mn}_{1.95}\text{Co(III)}_{0.05}\text{O}_{4.126}$			110	

ences in electrochemical behaviour between stoichiometric  $\text{LiMn}_2\text{O}_4$  and the metal-ion doped spinels occurs mainly in the high voltage region. The charge curves between 3.9 and 4.4 V are enlarged in Fig. 2B. It is evident that both types of compound have the same S-shaped curve at a capacity of less than at  $75 \text{ mAh g}^{-1}$  (region I); this corresponds to 0.5 M lithium ions per unit insertion or extraction. At capacities above  $75 \text{ mAh g}^{-1}$ , the metal-ion doped spinels still retain the S-shaped curves, while the shape of the charge curve for the stoichiometric spinel  $\text{LiMn}_2\text{O}_4$  becomes L-shaped. It is well-known that an S-shaped curve is characteristic of a one-phase reaction, and the L-shaped curve of a two-phase reaction [9]. Thus, the metal-ion doped spinels will provide a stable structure for the insertion/extraction of lithium ions during charge and discharge, and it is therefore expected that both the

room-temperature and the elevated-temperature performances will be improved.

To confirm this anticipation, cycling life tests of the  $\text{Li}/\text{LiMn}_2\text{O}_4$  system with all the above samples were conducted on CR2032 coin cells at room temperature. The rechargeable capacity of each sample is plotted in Fig. 3 as a function of cycle number. There is a slight fading of capacity for the metal-ion doped spinels. Almost no capacity loss is found with samples C and D, which have the smallest lattice cubic parameter (8.22–8.23  $\text{\AA}$ ) of all the compounds. The smaller spinel framework will provide a more reversible structure for lithium ion intercalation-deintercalation, and thereby will promote structural stability and arrest the loss of  $\text{MnO}$ , as observed. All the above results strongly support the conclusion that if there is a change in the structure, then  $\text{MnO}$  will be lost at room temperature.

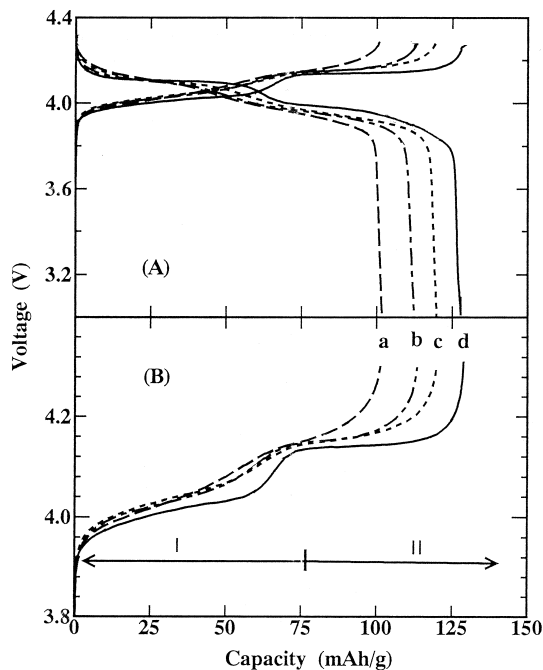


Fig. 2. Typical charge and discharge curves of  $\text{Li}/1 \text{ M LiPF}_6\text{-EC/DMC}$  (1:2 in volume)/ $\text{LiMn}_2\text{O}_4$  cells containing various spinel electrodes. (a) sample A; (b) sample B; (c) sample C, and (d) sample D. (B) Enlargement of charge curves in (A) between 3.8 and 4.3 V. Cells cycled at a current rate of  $C/3$  between 3.0 and 4.3 V. The data collected at room temperature.

### 3.3. Elevated-temperature performance

As mentioned in the introduction, change in the unstable two-phase accompanied by loss of  $\text{MnO}$  has been proposed to be a major factor in capacity retention cycling at elevated temperature. Accordingly, if the spinel electrode has a stable structure, then the elevated-temperature performance should be improved. To examine this proposition, the capacity retention of  $\text{LiMn}_2\text{O}_4$  was also compared

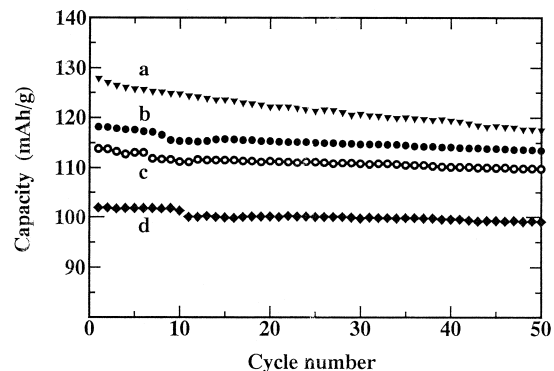


Fig. 3. Cycling behaviour of  $\text{Li}/1 \text{ M LiPF}_6\text{-EC/DME}$  (1:2 in volume)/ $\text{LiMn}_2\text{O}_4$  cells at room temperature with various spinel electrodes: (a) sample A; (b) sample B; (c) sample C; (d) sample D. Cells cycled at a current rate of  $C/3$  between 3.0 and 4.3 V.

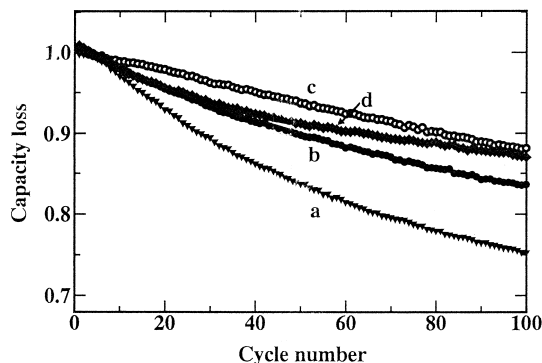
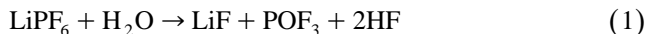


Fig. 4. Cycling behaviour of Li/1 M LiPF<sub>6</sub>-EC/DME (1:2 in volume)/LiMn<sub>2</sub>O<sub>4</sub> cells at 50°C with various spinel electrodes. (a) sample A; (b) sample B; (c) sample C; (d) sample D. Cells cycled at a current rate of  $C/3$  between 3.0 and 4.3 V.

with that of metal-ion doped spinels on cycling at 50°C, the results are shown in Fig. 4. LiMn<sub>2</sub>O<sub>4</sub> loses about 25% of its initial capacity over the first 100 cycles, compared with 17, 12 and 13% for samples B, C and D, respectively. Improving the elevated-temperature performance is interpreted in terms of the mechanism proposed at room temperature namely, a homogeneous reaction proceeds over the entire intercalated region for the metal-ion doped spinels and thus reduces Mn dissolution. With the fluorine-substituted spinel, the substitution of fluoride is also crucial towards improving the intrinsic structural stability of the spinels towards decomposition [10]. On other hand, spinel electrode can directly lose Mn<sub>2</sub>O<sub>3</sub> at a high temperature, which will further cause capacity loss. This would explain the fact that metal-ion doped spinels still lose capacity on cycling at elevated temperature. The corrosion rate may depend on both the electrolyte acidity and the nature of the surface of the electrode materials. LiPF<sub>6</sub> is very sensitive to moisture, and reacts to form HF, i.e.,



HF encourages Mn<sub>2</sub>O<sub>3</sub> to dissolve in the solution, and this suggests that a useful route to improving the elevated-tem-

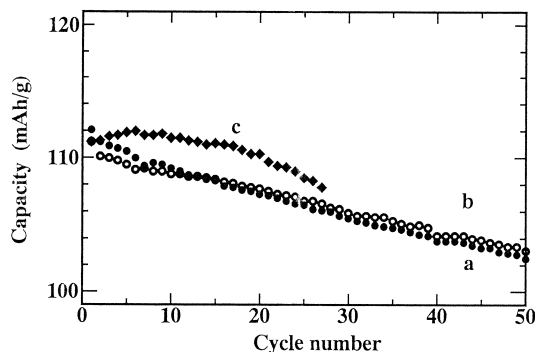


Fig. 5. Cycling behaviour of Li/organic electrolyte/Li<sub>1.04</sub>Mn<sub>1.95</sub>Co<sub>0.05</sub>O<sub>4</sub> cell in various electrolyte solutions at 50°C: (a) 1 M LiPF<sub>6</sub>-EC/DMC; (b) 1 M LiBF<sub>4</sub>-EC/DMC; (c) 1 M LiClO<sub>4</sub>-EC/DMC. Cells cycled at a current rate of  $C/3$  between 3.0 and 4.3 V.

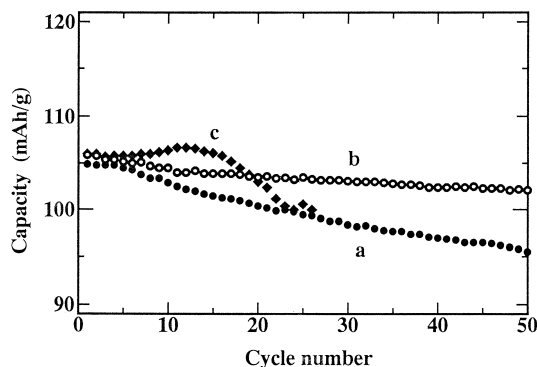


Fig. 6. Cycling behaviour of Li/organic electrolyte/Li<sub>1.10</sub>Mn<sub>1.95</sub>Co<sub>0.05</sub>O<sub>4</sub> cell in various electrolyte solutions at 50°C: (a) 1 M LiPF<sub>6</sub>-EC/DMC; (b) 1 M LiBF<sub>4</sub>-EC/DMC; (c) 1 M LiClO<sub>4</sub>-EC/DMC. Cells cycled at a current rate of  $C/3$  between 3.0 and 4.3 V.

perature performance is to reduce the HF content in the electrolyte solution.

### 3.4. Effect of electrolyte

In order to understand further the effect of the acidity on the capacity retention on cycling at elevated temperature, Li/LiMn<sub>2</sub>O<sub>4</sub> cells based on Li<sub>1.04</sub>Mn<sub>1.95</sub>Co<sub>0.05</sub>O<sub>4.053</sub> and Li<sub>1.1</sub>Mn<sub>1.95</sub>Co<sub>0.05</sub>O<sub>4.126</sub> electrodes were examined in 1 M LiClO<sub>4</sub>-EC/DMC and 1 M LiBF<sub>4</sub>-EC/DMC solutions. The specific capacity is plotted in Figs. 5 and 6 as a function of cycle number. It is clear that the elevated-temperature performance is improved in 1 M LiBF<sub>4</sub>-EC/DMC solution, specially for the Li<sub>1.1</sub>Mn<sub>1.95</sub>Co<sub>0.05</sub>O<sub>4.126</sub> electrode, while there is very little change for the Li<sub>1.04</sub>Mn<sub>1.95</sub>Co<sub>0.05</sub>O<sub>4.053</sub> electrode. This is probably because the LiBF<sub>4</sub> electrolyte is not acidic since it does not react with traces of moisture like LiPF<sub>6</sub>. The difference in the performance of the two electrode materials should be in part due to their different surface areas. In the case of the LiClO<sub>4</sub>-based electrolyte, it appears that the cells maintain capacity over the first 20 cycles, but then lose capacity

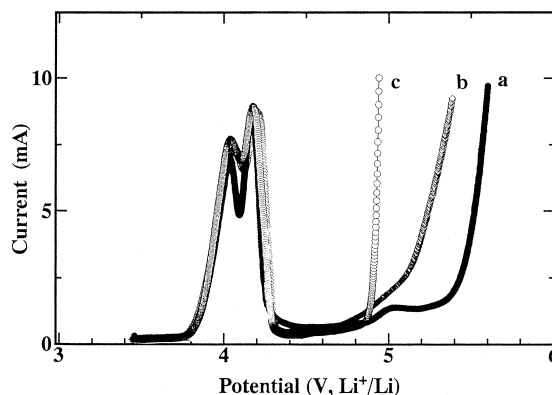


Fig. 7. Cyclic voltammograms for LiMn<sub>2</sub>O<sub>4</sub> in various electrolyte solutions: (a) 1 M LiPF<sub>6</sub>-EC/DMC; (b) 1 M LiBF<sub>4</sub>-EC/DMC; (c) 1 M LiClO<sub>4</sub>-EC/DMC. The data collected at 50°C.

rapidly. Careful inspection of the coin cell revealed that the electrolyte had evaporated from the cell. This is probably caused by decomposition of the electrolyte and consequent increase in the pressure in the cell. For all the above three electrolytes, the thermal and chemical stability are in the following order:  $\text{LiPF}_6 < \text{LiBF}_4 < \text{LiClO}_4$ . Although  $\text{LiClO}_4$  is known to be a strong oxidizing agent and generally exhibits very good electrochemical stability, catalytic effects at the spinel electrode may destabilize  $\text{LiClO}_4$  [11]. Cyclic voltammograms for the  $\text{LiMn}_2\text{O}_4$  electrode in the three electrolytes are given in Fig. 7. The decomposition potential on the spinel  $\text{LiMn}_2\text{O}_4$  electrode at  $50^\circ\text{C}$  is 4.92, 5.07 and 5.43 V ( $\text{Li}^+$  vs. Li metal) for  $\text{LiClO}_4$ ,  $\text{LiBF}_4$  and  $\text{LiPF}_6$ -based electrolyte, respectively.

### 3.5. Effect of surface area

It should be noted that the specific surface-area of the electrode material also exerts a major influence on the loss of Mn and decomposition of the electrolyte at elevated temperature. To evaluate the effect of surface area on the capacity loss during cycling, two samples E and F with the same chemical composition but with different surface area were cycled in Li/1 M  $\text{LiPF}_6$ -EC/DMC/ $\text{LiMn}_2\text{O}_4$  coin cells at  $50^\circ\text{C}$ . The chemical formula of samples E and F is  $\text{Li}_{1.1}\text{Mn}_2\text{O}_{4.19}$  and  $\text{Li}_{1.1}\text{Mn}_2\text{O}_{4.17}$ , respectively. Scanning electron micrographs given in Fig. 8 reveal that samples E and F have a mean particle size of 0.1 and 0.6  $\mu\text{m}$ ,

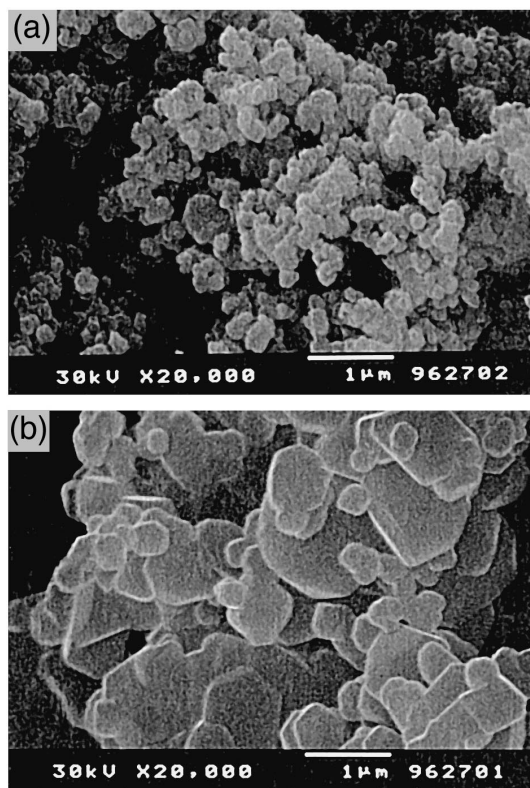


Fig. 8. Scanning electron micrographs of (a) sample E and (b) sample F.

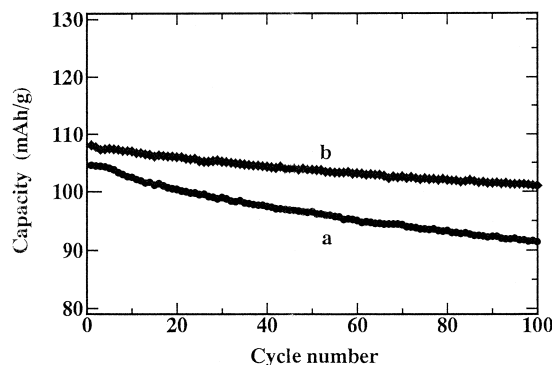


Fig. 9. Capacity as a function of cycle number for Li/1 M  $\text{LiPF}_6$ -EC/DME (1:2 in volume)/ $\text{LiMn}_2\text{O}_4$  cells at  $50^\circ\text{C}$  based on spinel electrodes with a surface area of (a)  $6.3 \text{ m}^2 \text{ g}^{-1}$  and (b)  $1.2 \text{ m}^2 \text{ g}^{-1}$ . Cells cycled at a current rate of  $C/3$  between 3.0 and 4.3 V.

respectively. The corresponding specific surface-area is  $6.3$  and  $1.2 \text{ m}^2 \text{ g}^{-1}$ . The spinel with the larger surface area loses about 12% of its initial capacity over 100 cycles, while that with the small surface area loses approximately half as much (Fig. 9). The improved elevated-temperature performance of the spinel with smaller surface area may be due to a reduction in the Mn dissolution and in the electrolyte decomposition. Studies are in progress to confirm this conclusion.

## 4. Conclusions

The elevated-temperature performance of metal-ion doped spinels has been improved. This is because they provide a stable structure for lithium-ion insertion/extraction during cycling and thereby, experience a reduced loss of MnO. The use of low acidity electrolyte solution, e.g.,  $\text{LiBF}_4$ , is also recommended as a means to arrest the dissolution of Mn.

## References

- [1] Y. Xia, H. Takeshige, H. Noguchi, M. Yoshio, J. Power Sources 56 (1995) 61.
- [2] Y. Xia, M. Yoshio, J. Power Sources 57 (1995) 125.
- [3] Y. Xia, M. Yoshio, J. Power Sources 63 (1996) 97.
- [4] R.J. Gummow, A. de Kock, M.M. Thackeray, Solid State Ionics 69 (1994) 59.
- [5] Y. Xia, M. Yoshio, J. Power Sources 66 (1997) 129.
- [6] Y. Xia, Y. Zhou, M. Yoshio, J. Electrochem. Soc. 144 (1997) 2593.
- [7] H. Kurimoto, K. Suzuoka, T. Murakami, Y. Xia, H. Nakamura, M. Yoshio, J. Electrochem. Soc. 142 (1995) 2178.
- [8] M. Yoshio, J. Taira, H. Noguchi, K. Isono, Denki Kagaku 66 (1998) 335.
- [9] Y. Xia, M. Yoshio, J. Electrochem. Soc. 143 (1996) 825.
- [10] G.G. Amatucci, A. Blyr, C. Schmutz, J.M. Tarascon, Prog. Batt. Batt. Mat. 16 (1997) 1.
- [11] H. Mao, J.N. Reamers, Q. Zhong, U. von Sacken, The Electrochemical Society Proceedings, in: S. Megahed (Ed.), Rechargeable Lithium and Lithium-ion Batteries, Vol. 94-28, p. 245.